Structural and Dielectric Properties of $CuCl_2$ and $ZnCl_2$ Doped Polyaniline

Ersel Ozkazanc,[1] Sibel Zor,[2] Hatice Ozkazanc[2]
[1]*Department of Physics, Kocaeli University, Kocaeli 41380, Turkey*

[2]*Department of Chemistry, Kocaeli University, Kocaeli 41380, Turkey*

This article addresses the synthesis and characterization of polyaniline (PANI) both in pure and doped forms with various levels of $CuCl_2$ and $ZnCl_2$ in HCl medium where ammonium persulphate was used as an oxidant. Synthesized polymeric materials were characterized spectroscopically (UV-visible spectroscopy, Fourier transform infrared spectroscopy, and Atomic absorption spectroscopy), thermally (Differential scanning calorimetry), and morphologically (Scanning electron microscopy). Free adsorption energy was calculated via Langmuir adsorption isotherm based on the quantities of Cu^{2+} and Zn^{2+} cations in both pre- and post- polymerization process where it was found that Cu^{2+} and Zn^{2+} are adsorbed physically on PANI surface. The dielectric measurements as a function of frequency and temperature showed that conductivity decreased with increasing doping levels of metal cations at high temperatures. POLYM. COMPOS., 31:1862–1868, 2010.

INTRODUCTION

Conducting polymers have widely been investigated in the last two decades due to their unique electrical properties and potential applications in various electronic devices, such as sensors, light emitting diodes, and rechargeable batteries [1–17]. Among the conducting polymers, polyaniline (PANI) is one of the most popular for its easy synthesis, high electrical conductivity, and good environmental stability [1, 3, 6–10, 12–37]. PANI is available in four different forms, such as leucoemeraldine base (colorless), emeraldine base (blue), pernigraniline base (violet), and emeraldine salt (green) depending on the pH of the solution and oxidation potential out of which only emeraldine salt (or protonated emeraldine) is electrically conducting. It can easily be synthesized through electrochemical or chemical oxidation of aniline with the help of oxidants like ammonium peroxidisulphate in acidic medium [1, 5, 6, 9, 10, 18, 23–26, 28, 31, 33, 35–37].

Correspondence to: E. Ozkazanc; e-mail: erseloz@kocaeli.edu.tr
DOI 10.1002/pc.20979
Published online in Wiley Online Library (wileyonlinelibrary.com).

There has been a considerable effort in recent years towards improving structural and physical properties of conducting polymers synthesized with various methods and doping processes [2, 4, 6–8, 14–19, 29, 30, 33, 34]. In this study, the synthesis of PANI in pure form as well as doped with $CuCl_2$ and $ZnCl_2$ at various levels were carried out by using a simple and low-cost chemical method where ammonium persulphate $(NH_4)_2S_2O_8$ was used as an oxidant for aniline. We first reported results of Fourier transform infrared spectroscopy (FTIR) and UV-visible (UV-vis) spectroscopy. Different to the literature, we then reported quantities of Cu^{+2} and Zn^{2+} remained in filtrate before and after the chemical polymerization determined by using atomic absorption spectroscopy (AAS). The adsorption of metal cations adsorbed to PANI surface was examined by Langmuir adsorption isotherm. Finally, Scanning electron microscopy (SEM), Differential scanning calorimetry (DSC), and dielectric measurements were performed.

EXPERIMENTAL

Synthesis of Polyaniline

PANI was synthesized with chemical oxidation polymerization where ammonium persulphate (Merck, Germany) was used as an oxidant. Aniline (5 mL) was dissolved in 1.5 M, 70 mL HCl (Merck, Germany), 10 g of $(NH_4)_2S_2O_8$ dissolved in 20 mL deionized water was subsequently added into the above solution. The whole solution was stirred at a constant speed for 5 hrs at a constant temperature of 25°C. After the polymerization, the whole solution was filtered, washed, and dried leading to green emeraldine salt form of PANI granules.

Doping Process

$CuCl_2$ and $ZnCl_2$ (Merck, Germany) salts of various doping levels of 2, 6, and 10% each prepared in 5 mL deionized water is added into the polymerization solution

prepared as described in the earlier paragraph just before the stirring stage. The whole solution was again stirred at a constant speed and a constant temperature of 25°C for 5 hrs. After the polymerization, the whole solution was again filtered, washed, and dried leading to doped PANI samples.

Measurements

Infrared spectra were carried out using a Shimadzu FTIR 8201 spectrophotometer in the range from 4000–400 cm^{-1} in KBr pellets. UV-vis spectra were measured in the wavelength region of 200–1000 nm using an Agilent UV-vis spectrometer. The DSC analyses were performed using a Mettler Toledo DSC 1 in the temperature range of 200–700 K with a heating rate of 5 $Kmin^{-1}$. Philips XL30SFEG SEM-EDX scanning electron microscope, operating at an accelerating voltage of 20 kV was used to observe the morphology of the samples. Quantities of Cu^{2+} and Zn^{2+} in 5 mL 2%, 6, 8, and 10% $CuCl_2$ and $ZnCl_2$ solution before the polymerization process were measured with atomic absorption spectrometer (Perkin Elmer AA-Analyst 800). The deionized water solutions used to wash the PANI samples after the polymerization were collected and Cu^{2+} and Zn^{2+} quantities in these solutions were also measured in the same way. These solutions were diluted hundred times during the measurements.

For the dielectric measurements, the surfaces of the samples were covered with silver paste to form electrodes. The dielectric measurements were performed between 10 kHz and 1 MHz frequency range at different temperatures (300–400 K) by using an LCR meter (Agilent 4284A). The real (dielectric constant, ε') and imaginary (or loss index, ε'') parts of the complex dielectric constant were calculated by using following equations:

$$\varepsilon' = \frac{C_p d}{\varepsilon_0 A} \tag{1}$$

$$\varepsilon'' = \varepsilon' \, tan \, \delta \tag{2}$$

where C_p is the capacitance of the sample; ε_0 (dielectric permittivity in vacuum) is equal to 8.85×10^{-14} F/cm; A is the effective surface area of the electrode; and d is the thickness of the sample. Ac-conductivities (σ_{ac}) of the samples were calculated with the help of *Eq. (3)*.

$$\sigma_{ac} = \frac{\omega C_p d \, tan \, \delta}{A} \tag{3}$$

where ω is the angular frequency ($2\pi f$).

RESULTS AND DISCUSSION

Fourier Transform Infrared Spectroscopy

In all FTIR spectra shown in Fig. 1, characteristic peaks of PANI can be clearly seen.

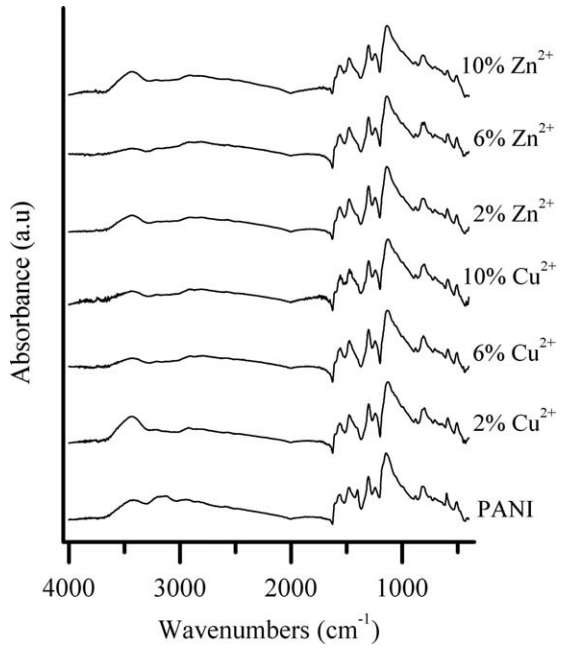

FIG. 1. FTIR absorbance spectra of $CuCl_2$ and $ZnCl_2$ doped PANI.

It is seen that N—H stretching at weak absorbance is within the range of 3650–3100 cm^{-1} and C—H stretching is within the range of 3100–2800 cm^{-1} [2, 3, 4, 9, 14–18, 25, 33, 34]. Aromatic ring stress, N—H deformation and C=N stretching gives absorption in the region from 1600 up to 1450 cm^{-1} [15, 21, 22, 30]. The peaks at 1559 and 1478 cm^{-1} are related to quinine and benzene ring stress deformation, respectively [7, 9, 17, 21, 25].

The band characteristics of the emeraldine salt form (or conducting protonated form) are observed at 820, 1144, 1244, and 1304 cm^{-1}. These bands are assigned to the vibration mode of the $—NH^+=$ structure, which is formed during the protonation of imine sites [9, 16, 18, 20, 21, 25, 35].

Spectrum peaks of 2, 6, and 10% Cu^{2+} and Zn^{2+} doped and pure PANI are within the similar reported ranges. However, slight shifts are observed in the wavelengths of the peaks upon the addition of Cu^{2+} and Zn^{2+} as tabulated in Table 1.

As it can be seen, quinoid and benzenoid peaks forming the main peaks of the spectrum have shifted upon the addition of 10% Cu^{2+} when compared to pure PANI from 1559 cm^{-1} to 1557 cm^{-1} and from 1478 cm^{-1} to 1474 cm^{-1}, respectively. The quinoid peak has also shifted to 1564 cm^{-1} from 1559 cm^{-1} following 10% Zn^{2+} addition compared to pure PANI. These shifts in the FTIR spectrum upon the addition of Cu^{2+} and Zn^{2+} is thought to be due to interactions between PANI and metal cations.

UV-visible spectroscopy

Figure 2 shows UV-visible absorption spectra at various doping levels of Cu^{2+} and Zn^{2+} as well as pure PANI samples.

TABLE 1. IR band assignments of PANI doped at various levels of $CuCl_2$ and $ZnCl_2$.

Frequency (cm^{-1})							
PANI	PANI/Cu^{2+} (2%)	PANI/Cu^{2+} (6%)	PANI/Cu^{2+} (10%)	PANI/Zn^{2+} (2%)	PANI/Zn^{2+} (6%)	PANI/Zn^{2+} (10%)	Assignment
820	800	806	801	812	816	814	C—H stretching
1144	1127	1132	1127	1138	1140	1136	C=C quinoide ring
1244	1242	1242	1242	1242	1242	1242	C—N stretching
1304	1300	1302	1300	1302	1302	1302	C—N stretching
1478	1478	1476	1474	1476	1476	1478	C=C benzoide ring
1559	1561	1557	1557	1561	1559	1564	C=C quinoide ring
2940	2924	2914	2913	2911	2914	2911	C—H stretching
3424	3428	3424	3443	3432	3422	3428	N—H stretching

PANI's characteristic absorption bands are observed at approximately 300, 450, 650, and 780 nm. The band observed in approximately 300 nm in all samples is related to the π-π^* transitions of aniline or aniline radicals [6, 9, 20, 22, 32, 33]. The absorption band observed in approximately 450 nm in all spectrum curves belongs to π-π^* transitions of quinine-iminium ions or polaron- π^* transitions [22, 34]. Due to the π-π^* transitions of quinine-imin groups, absorption bands are formed in 600–660 nm [3, 6, 9, 22, 32]. The absorption bands around 450 and 780 nm belong to conducting emeraldine salt form of the PANI [5, 19, 33, 35, 37].

Atomic Absorption Spectroscopy

The chemical polymerization reaction using ammonium persulphate as an oxidant is shown in Fig. 3.

According to the reaction mechanism, it is thought that the metal cations are adsorbed onto the molecule surface because of the electrostatic interaction with Cl^- ions. It is therefore thought that Cu^{2+} and Zn^{2+} cations added during the chemical polymerization do not enter into a chemical reaction with PANI molecules.

The quantity of metal cations adsorbed onto the PANI molecule surface was determined to obtain appropriate adsorption isotherm, through which adsorption free energy was calculated. Various adsorption isotherms were tried and Langmuir adsorption isotherm was found to be the most appropriate adsorption isotherm [37–44]. Langmuir adsorption isotherm is given by the following expression;

$$ln\frac{\theta}{1-\theta} = lnC + ln\,K \tag{4}$$

where C is the concentration of metal cations ($mol.dm^{-3}$) and K is the adsorption equilibrium constant. Θ is the surface fraction of the metal cations that are adsorbed on the molecule surface as determined by *Eq. (5)*:

$$\theta = \frac{C_0 - C}{C} \tag{5}$$

where C_0 is the quantity of 5 mL 2, 6, 8, and 10% Cu^{2+} and Zn^{2+} cations in ppm before the chemical polymerization. C is the quantity of Cu^{2+} and Zn^{2+} cations in ppm remained at the filtrate after the chemical polymerization. The change of $ln\frac{\theta}{1-\theta}$ with respect to lnC for Cu^{2+} and Zn^{2+} is given in Fig. 4. Adsorption equilibrium constant K was determined using the slope of isotherm curve.

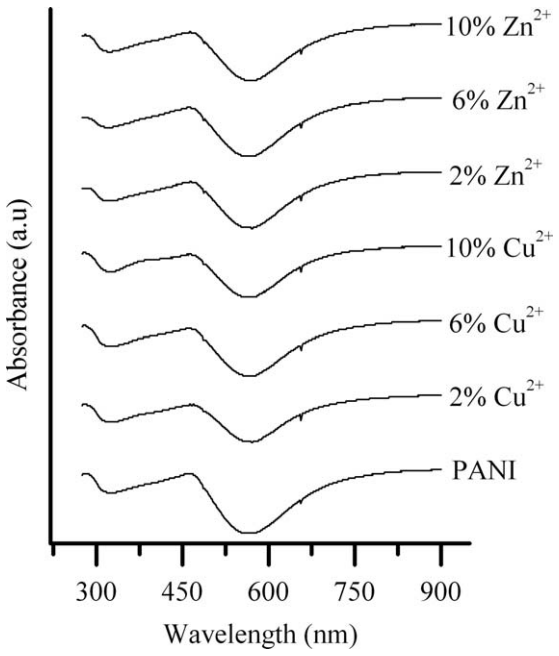

FIG. 2. UV-vis spectra of $CuCl_2$ and $ZnCl_2$ doped PANI.

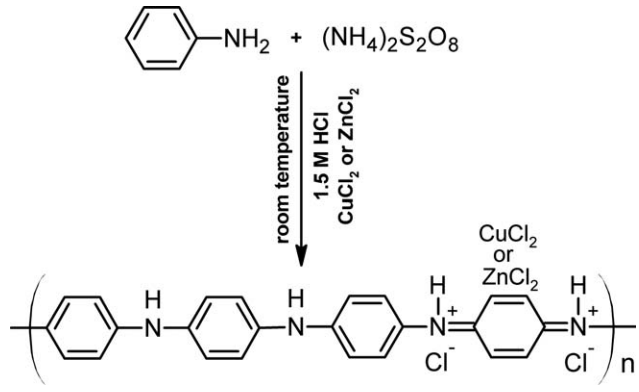

FIG. 3. The reaction mechanism of $CuCl_2$ and $ZnCl_2$ doped PANI.

 DOI 10.1002/pc

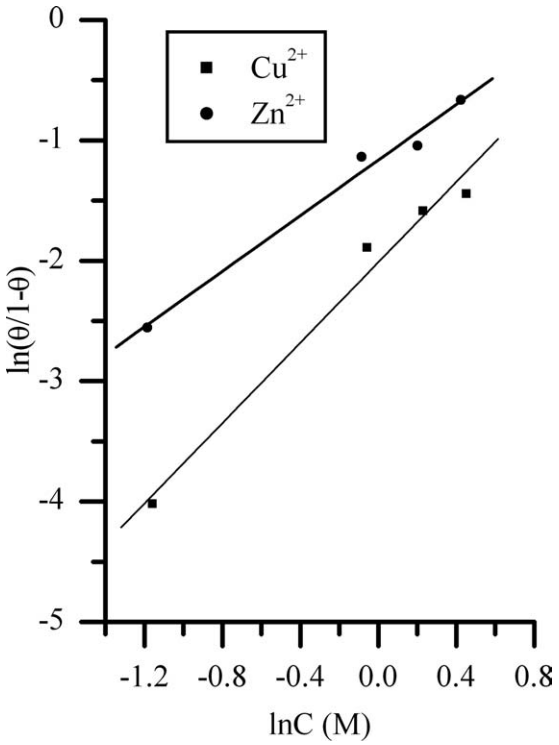

FIG. 4. Langmuir adsorption isotherm plots of PANI doped various levels of metal cations.

Putting the calculated K value into *Eq. (6)* allows us to calculate adsorption free energy, ΔG^0_{ads};

$$K = \frac{1}{55.5} exp(-\frac{\Delta G^0_{ads}}{RT}) \quad (6)$$

The constant number, 55.5 is the concentration of water in the solution (mol dm^{-3}). The calculated ΔG^0_{ads} values for Cu^{2+} and Zn^{2+} are -4.960 and -7.067 kJ/mol, respectively. The negative value of ΔG^0_{ads} shows that the reaction is realized spontaneously [38, 41–44]. The adsorption type is generally regarded as physisorption if the change of free energy (ΔG^0_{ads}) is between -20 and 0 kJ/mol. The adsorption behavior is attributed to the electrostatic interaction between the metal cations and polymer surface. When the value of ΔG^0_{ads} is between -80 and -400 kJ/mol, the adsorption would be considered as chemisorption [41, 42, 44]. It is clear from these results that the adsorption mechanism of metal cations is typical physisorption.

Scanning Electron Microscopy

Figure 5 shows scanning electron micrographs of pure and $CuCl_2$ and $ZnCl_2$ doped PANI samples. Pure PANI includes local heterogeneous regions according to particle size [Fig. 5(a)]. However, absence of pores in the structure shows that there is a very strong interaction among the particles. The conductivity is provided by the mobility of charge carriers in such structures and it is closely related to interparticle connection. It is then reasonable to conclude that pure PANI has a conductive nature.

As seen in Figs. 5b and c, the structure of $CuCl_2$ and $ZnCl_2$ doped PANI is more homogenous, the particle size dispersion is narrower and the image is brighter (i.e. no noise). The brightness is due to the higher electron efficiency coming from the surfaces of the samples which could be attributed to higher conductivity of doped PANI samples.

Differential Scanning Calorimetry

Sharp endotherm peak seen at about 410 K in DSC thermograms given in Fig. 6 for PANI samples is a characteristic peak associated with moisture, which appears after the separation of HCl from the structure.

The other sharp endotherm peak seen at approximately 610 K for pure PANI shows a thermal degradation (T_d)

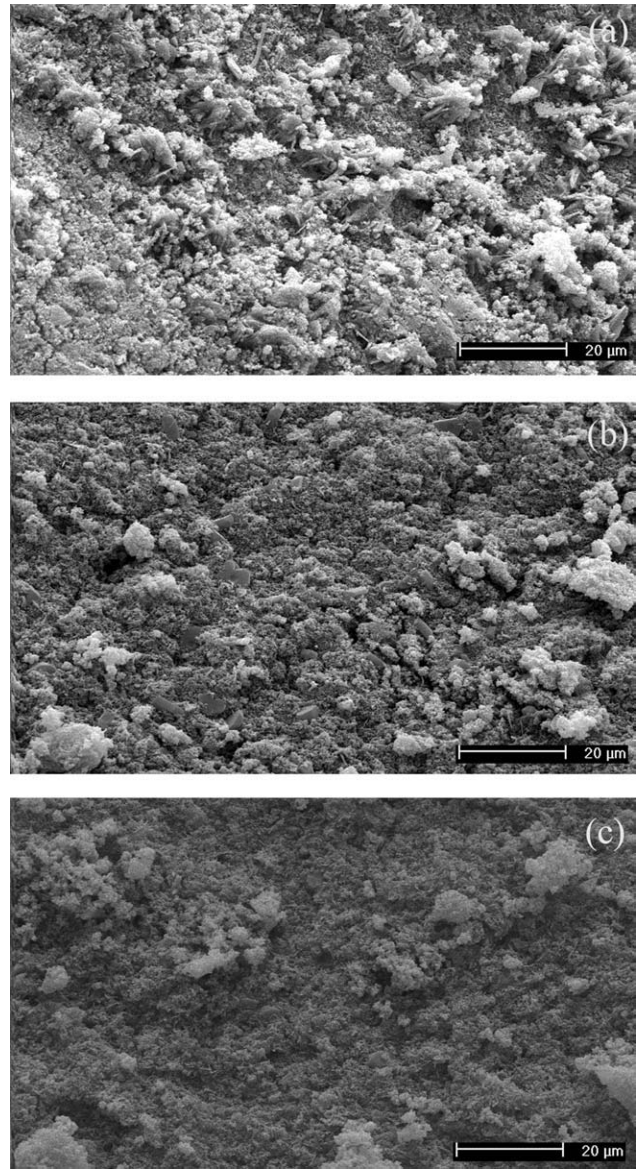

FIG. 5. Scanning electron micrographs of (a) Pure PANI, (b) PANI-$CuCl_2$ (2%), and (c) PANI-$ZnCl_2$ (2%).

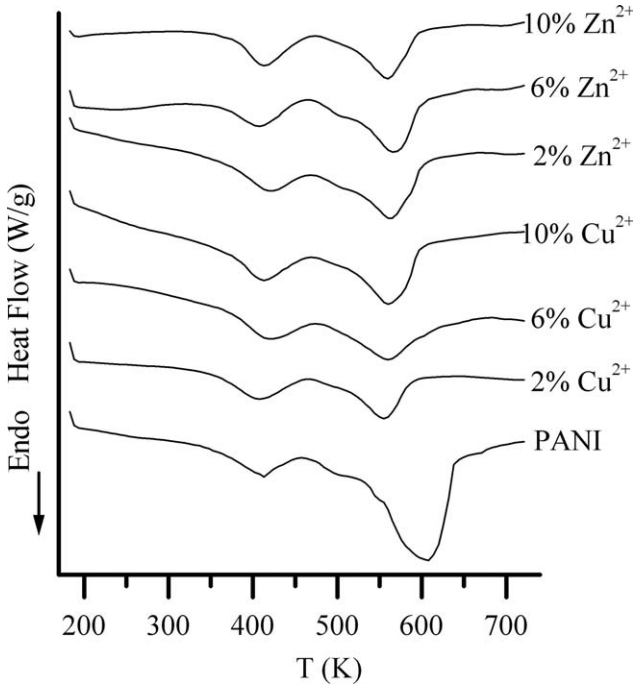

FIG. 6. DSC thermograms of $CuCl_2$ and $ZnCl_2$ doped PANI.

associated with the cross bonds [3, 10, 31, 32]. As seen from the Fig. 6, the T_d value for Cu^{2+} and Zn^{2+} doped PANI samples shifts to about 560 K. The onset of thermal degradation with the doping process at a lower temperature shows that the metal cations adsorbed onto the molecule surface are more easily affected. The pure PANI which is in a more stable structure starts to degrade at higher temperatures as expected. Furthermore, it is not surprising that the most intense peak for degradation temperature, T_d belongs to the pure PANI. That is because; the pure PANI absorbs more thermal energy during the degradation when compared to the samples containing Cu^{2+} and Zn^{2+} cations.

Dielectric Measurements

The dielectric response is generally explained by real (ε') and imaginary (ε'') parts of complex dielectric constant. ε' and ε'' components are associated with the storage and loss of energy in the external field. The change of dielectric characteristics of PANI sample in pure form at different temperatures and frequencies is given in Fig. 7.

As seen in Fig. 7, both ε' and ε'' tend to decrease with the frequency increase for all temperatures. It can be seen that real part increases at relatively lower frequencies and starts to decrease as the frequency goes higher. This is one of the characteristic properties of conducting polymers [11]. The real part, ε' reaches to rather large values at lower frequencies depending on the temperature increase. This is usually the result of intersurface interactions within the material as well as electrode effects [8, 15, 24, 29]. The increase that takes place in free volume at higher temperatures facilitates easier move of dipole components, hence leading to a higher dielectric constant.

Figure 8 shows how real part is affected by different doping levels for a number of temperatures at 1 MHz constant frequency.

The increase which is seen in real part for 300 K in both $CuCl_2$ and $ZnCl_2$ doped samples shows that the doping process increases the total dipole momentum of the structure. The decrease occurred in the free volume upon doping does not seem to reach the level that can affect the movement of dipoles associated with N and Cl at approximately room temperature. However, towards the higher temperatures, the increase in real part starts to ease off.

It is expected that dipoles would be more active with increasing temperatures due to increased thermal activity, therefore resulting in an increased real part. However, dipolar mobility under an external field would be lower as electrostatic interaction at these temperatures is weaker. Hence, the rate of increase in total dipole moment would tend to slow down with increasing temperatures.

The dielectric constant and conductivity levels of the polymers are important considerations in a possible technological application. Figure 9 shows the behavior of *ac* conductivity of pure PANI as a function of temperature at two frequencies.

Conductivity of pure PANI shows a sharp increase of approximately 10 times after 360 K. Thermal mobility at higher temperatures increases significantly, therefore charge carriers are able to move more easily within the structure giving rise to higher conductivity values. Figure 10 shows the effect of doping process on *ac* conductivity for different temperatures at 1 MHz constant frequency.

As seen from Fig. 10, the conductivity behavior of samples doped with both $CuCl_2$ and $ZnCl_2$ is almost the

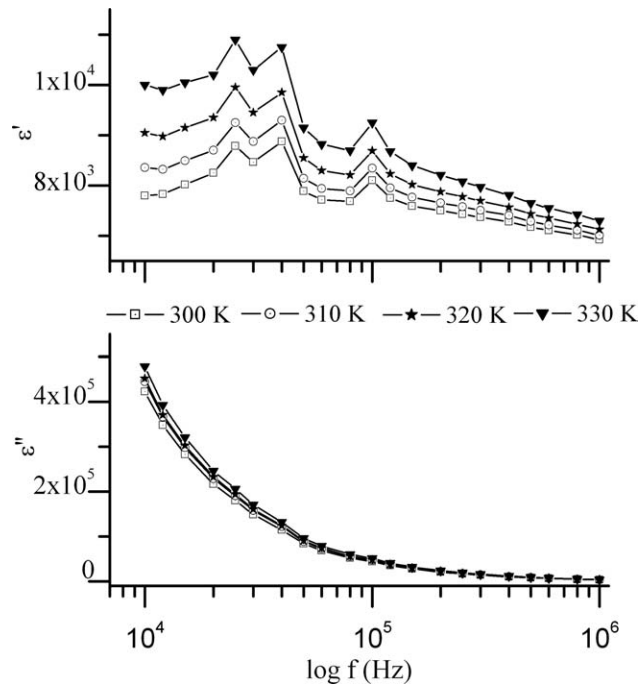

FIG. 7. Frequency dependent variations of real and imaginary parts of complex dielectric constant at different temperatures for pure PANI.

 DOI 10.1002/pc

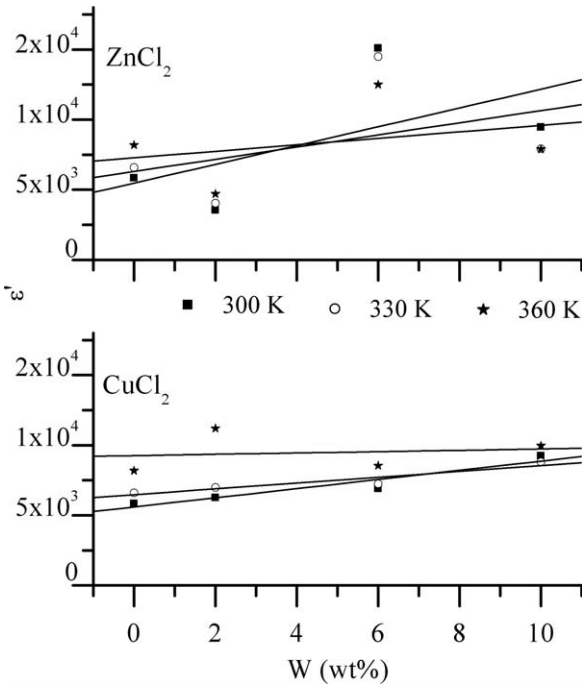

FIG. 8. Variation of real part depending on the doping level at different temperatures for 1 MHz constant frequency.

same. There is an increasing trend with doping level at 300 K. However, while there is no significant effect of the doping level is observed at 350 K, a noticeable decrease is seen in *ac* conductivity at 400 K.

It is known that the conductivity is characterized by the activity of charge carriers. The adsorption results obtained in this study reveals a weak electrostatic interaction between PANI and metal cations. When considering the earlier, the effect of doping process on the conductivity at relatively higher temperatures is not surprising. The mobility of charge carriers under an external field at around 300 K increases with the doping level. It is normally expected that charge carriers moving more easily at higher temperatures lead to an increased conductivity. However, it is seen that the thermal activity as a result of the temperature increase do not cause an important effect. The mobility of charge carriers is rather restricted due to doping process combined with electrostatic and thermal effects. Hence, the conductivity has decreased with increasing doping levels at higher temperatures as mentioned above.

CONCLUSIONS

Various levels of $CuCl_2$ and $ZnCl_2$ by weight were doped into emeraldine salt form of PANI, which was synthesized via a chemical method. The samples were investigated by using different techniques, such as FTIR, DSC-UV-vis, and SEM. Cu^{2+} and Zn^{2+} cation quantities in the solutions were determined by atomic absorption. The dielectric properties at different temperatures and frequencies were also studied.

Adsorption free energy calculated by Langmuir adsorption isotherm curve showed that binding between PANI and metal cations is not chemical but a weak electrostatic interaction.

It was determined from DSC thermograms that thermal degradation temperature (T_d) around 610 K belonging to pure PANI shifted to around 560 K for Cu^{2+} and Zn^{2+} doped PANI samples.

Dielectric measurement results of pure PANI showed that real part increased with increasing temperatures at

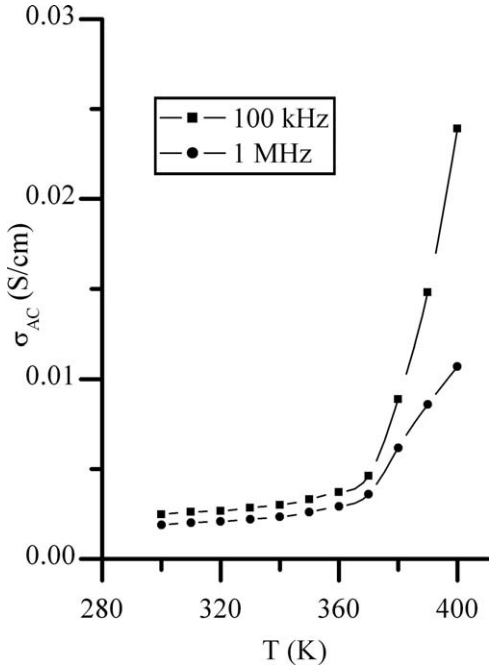

FIG. 9. Temperature dependent variations of ac conductivity at certain frequencies for pure PANI.

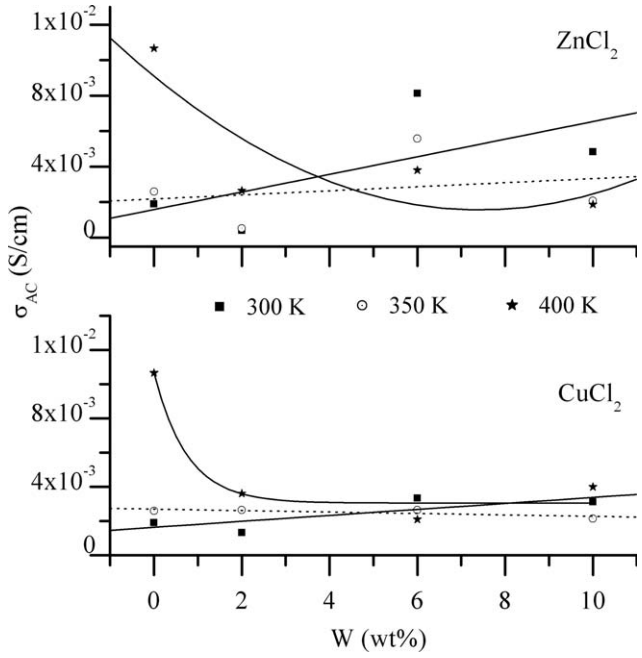

FIG. 10. Variation of ac conductivity depending on the doping level at different temperatures.

relatively low frequencies as a result of intersurface interactions and electrode effects. The effect of doping process on the real part was an increase up to the room temperature. However, due to the thermal activity at higher temperatures and with increasing doping level, the average dipole moment of the structure decreased. Therefore, the increase observed in the real part begins to slow down significantly at higher temperatures.

A similar behavior exists in the ac conductivity of the samples. Conductivity of pure PANI has shown a sharp increase after approximately 360 K whereas the conductivity of doped samples increased at around room temperature depending on the doping level. However, the increase slows down at higher temperatures and decreases significantly at around 400 K.

The conductive and dielectric properties of doped PANI samples have shown interesting properties as a function of temperature depending on the doping process could pave the way to better structured PANI composites for different technological applications.

ACKNOWLEDGMENT

The authors thank to Dr Ümit Ay for helping AAS measurements.

REFERENCES

1. M.S. Freund and B. Deore, *Self-Doped Conducting Polymers*, John Wiley & Sons Ltd, West Sussex, England (2007).
2. G.M. Neelgund, E. Hrehorova, M. Joyce, and V. Bliznyuk, *Polym. Int*., **57**, 1083 (2008).
3. P. Ghosh, A. Chakrabarti, and S.K. Siddhanta, *Eur. Polym. J*., **35**, 803 (1999).
4. V. Ali, R. Kaur, N. Kamal, S. Singh, S.C. Jain, H.P.S. Kang, M. Zulfequar, and M. Husain, *J. Phys. Chem. Solids*., **67**, 659 (2006).
5. T. Hino, T. Namiki, and N. Kuramoto, *Synth. Met*., **156**, 1327 (2006).
6. P. Saini, R. Jalan, and S.K. Dhawan, *J. Appl. Polym. Sci*., **108**, 1437 (2008).
7. N. Parvatikar, S. Jain, C.M. Kanamadi, B.K. Chougule, S.V. Bhoraskar, and M.V.N. Ambika Prasad, *J. Appl. Polym. Sci*., **103**, 653 (2007).
8. P. Dutta, S. Biswas, and S.K. De, *Mater. Res. Bull*., **37**, 193 (2002).
9. E.T. Kang, K.G. Neoh, and K.L. Tan, *Prog. Polym. Sci*., **23**, 277 (1998).
10. M.J.R. Cardoso, M.F.S. Lima, and D.M. Lenz, *Mater. Res*., **10**, 425 (2007).
11. M.G. Han and S.S. Im, *J. Appl. Polym. Sci*., **82**, 2760 (2001).
12. M.K. Ram, S. Annapoorni, S.S. Pandey, and B.D. Malhotra, *Polymer*, **39**, 3399 (1998).
13. S.A. Travain, G.F.L. Ferreira, J.A. Giacometti, and R.F. Bianchi, *Mater. Sci. Eng. B*, **143**, 31 (2007).
14. S. Ameen, V. Ali, M. Zulfequar, M.M. Haq, and M. Husain, *Phys. B* , **403**, 2861 (2008).
15. A. Sarkar, P. Ghosh, A.K. Meikap, S.K. Chattopadhyay, S.K. Chatterjee, P. Chowdhury, K. Roy, and B. Saha, *J. Appl. Polym. Sci*., **108**, 2312 (2008).
16. H. Narayan, H. Alemu, and E. Iwuoha, *Phys. Status. Solidi. A*, **203**, 3665 (2006).
17. T. Machappa and M.V.N. Ambika Prasad, *Phys. B: Condens Matter*, **404**, 4168 (2009).
18. R.M.G. Rajapaske, D.M.M. Krishantha, D.T.B. Tennakoon, and H.V.R. Dias, *Electrochim. Acta*., **51**, 2483 (2006).
19. H.-S. Kim, H.L. Hobbs, L. Wang, M.J. Rutten, and C.C. Wamser, *Synth. Met*., **159**, 1313 (2009).
20. Y.F. Huang and C.W. Lin, *Polymer*, **50**, 775 (2009)
21. S. Quillard, G. Louarn, J.P. Buisson, M. Boyer, M. Lapkowski, A. Pron, and S. Lefrant, *Synth. Met*., **84**, 805 (1997).
22. E. Erdem, M. Karakişla, and M. Saçak, *Eur. Polym. J*., **40**, 785 (2004).
23. R. Singh, V. Arora, R.P. Tandon, A. Mansingh, and S. Chandra, *Synth. Met*., **104**, 137 (1999).
24. B.G. Soares, M.E. Leyva, G.M.O. Barra, and D. Khastgir, *Eur. Polym. J*., **42**, 676 (2006).
25. I. Šedênková, M. Trchová, N.V. Blinova, and J. Stejskal, *Thin. Solid. Films*., **515**, 1640 (2006).
26. I. Sapurina and J. Stejskal, *Polym. Int*., **57**, 1295 (2008).
27. C. Basavaraja, R. Pierson, T.K. Vishnuvardhan, and D.S. Huh, *Eur. Polym. J*., **44**, 1556 (2008).
28. N.J. Pinto, A.A. Acosta, G.P. Sinha, and F.M. Aliev, *Synth. Met*., **113**, 77 (2000).
29. C.-H. Ho, C.-D. Liu, C.-H. Hsieh, K.-H. Hsieh, and S.-N. Lee, *Synth. Met*., **158**, 630 (2008).
30. B.K. Sharma, A.K. Gupta, N. Khare, S.K. Dhawan, and H.C. Gupta, *Synth. Met*., **159**, 391 (2009).
31. C.-H. Chen, *J. Appl. Polym. Sci*., **89**, 2142 (2003).
32. H.S.O. Chan, S.C. Ng, W.S. Sim, K.L. Tan, and B.T.G. Tan, *Macromolecules*, **25**, 6029 (1992).
33. P.P. Sengupta, P. Kar, and B. Adhikari, *React. Funct. Polym*., **68**, 1103 (2008).
34. S. Zhou, T. Wu, and J. Kan, *J. Appl. Polym. Sci*., **106**, 652 (2007).
35. X. Li and X. Li, *Mater. Lett*., **61**, 2011 (2007).
36. R. Singh, V. Arora, R.P. Tandon, and S. Chandra, *J. Mater. Sci*., **33**, 2067 (1998).
37. E. Detsri and S.T. Dubas, *J. Met. Mater. Miner*., **19**, 39 (2009).
38. X.-G. Li, H. Feng, and M.-R. Huang, *Chem. Eur. J*., **15**, 4573 (2009)
39. A.-N. Chowdhury, F.S. Saleh, M.R. Rahman, and A. Rahim, *J. Appl. Polym. Sci*., **109**, 1764 (2008).
40. M.A. Sharaf, H.A. Arida, S.A. Sayed, A.A. Younis, and A.B. Farag, *J. Appl. Polym. Sci*., **113**, 1335 (2009).
41. N. Tekin, Ö. Demirbaş, and M. Alkan, *Microporous Mesoporous Mater*., **85**, 340 (2005).
42. A.S. Özcan, B. Erdem, and A. Özcan, *Colloid Surf. A*., **266**, 73 (2005).
43. D. Kavitha and C. Namasivayam, *Bioresour. Technol*., **98**, 14 (2007).
44. K.F. Khaled and M.M. Al-Qahtani, *Mater. Chem. Phys*., **113**, 150 (2009).